Hysteretic behavior induced by an electroacoustic feedback loop in a thermo-acousto-electric generator

Gaelle Poignand, C. Olivier, Guillaume Penelet, Pierrick Lotton

Hysteretic behavior induced by an electroacoustic feedback loop in a thermo-acousto-electric generator

G. Poignand, C. Olivier, G. Penelet, P. Lotton

Laboratoire d'Acoustique de l'Université du Maine, UMR CNRS 6613, Avenue Olivier Messiaen, 72085 LE MANS Cedex 9, France.

Abstract

An active control method of the spatial distribution of the acoustic field is applied in a thermo-acousto-electric generator. An auxiliary acoustic source is used to force the self-sustained thermoacoustic oscillation in order to control the thermoacoustic amplification. The auxiliary source consists of a loudspeaker, located inside the loop-tube close to the main ambient heat exchanger, and supplied with a delayed signal through an electric feedback loop, comprising a phase-shifter and an amplifier, connected to a reference microphone. Experiments are performed on a prototype engine working with air at a static gauge pressure of 5 bars. Experimental results demonstrate how it is possible to tune the acoustic oscillations in order to increase the global performance of the generator, compared to the case without control, as well as the existence of a hysteretic behavior induced by the electroacoustic feedback loop itself, which leads to a discrepancy between the onset heat input and the offset one.

Keywords: Thermoacoustics, Heat engine, Acoustic field, Loudspeakers, Forced oscillations

1. Introduction

The thermoacoustic effect relies on the interaction between a porous material submitted to a temperature gradient and an oscillating gas, which leads to

Email address: gaelle.poignand@univ-lemans.fr (G. Poignand)

the onset of self-sustained acoustic oscillations. Such an interaction can be used to build thermoacoustic engines, a kind of piston-free thermodynamic engines which convert thermal power into acoustic power. In 1999, Backhaus and Swift [1] made a significant contribution by proposing a specific design of a thermoacoustic engine able to achieve a high thermoacoustic efficiency of 30% (41% of Carnot efficiency). The geometry of this engine, a torus-shaped waveguide attached to a resonator, provides the required acoustic field in the porous material (referred to as the regenerator) to achieve a Stirling cycle. More recently, an engine with a similar design built by Tijani et al. [2] reached a record efficiency of 32 % (49% of Carnot efficiency). Besides the possibility to achieve a high efficiency, thermoacoustic engines have a simple construction with no moving parts and they usually operate with inert gases which are environmentally friendly. These advantages compared to conventional engines make them attractive in a wide variety of applications. In particular, a thermoacoustic Stirling engine can be coupled to an alternator in order to produce green electricity from waste heat recovery. In such a device, called a Thermo-Acousto-Electric Generator (TAEG), the engine transforms the available heat into acoustic power which is further converted into electrical power via the alternator. Since the first TAEG built by Backhaus et al. [3] producing 60 W of electric power with an efficiency of 18%, other prototypes have been developed to address various requirements, such as the decrease of the onset temperature [4] to meet the need for waste heat recovery at low temperature, or the electricity production from a few watts with a low cost [5, 6], up to several kW [7] for energy recovery from industrial waste heat sources or solar source.

Tools [8] and methodologies [9] used to design or to predict the operation of thermoacoustic engines are based on the linear thermoacoustic theory established by Rott [10]. However, although the linear theory can accurately predict the onset of the thermoacoustic instability [11], this theory fails to predict the acoustic wave saturation at high amplitudes, which is governed by complex nonlinear processes. These nonlinear processes can affect the engine operation by dissipating acoustic power (through cascade process of higher harmonics gen-

eration [12, 13] or minor losses due to geometrical singularities [14, 15]) or by modifying the temperature field distribution (through acoustically induced thermal conductivity [10] or acoustic streaming [16, 17, 18, 19, 20]). For this last mechanism, Penelet et al. [21] have shown that a change in the shape of the temperature field leads to a modification of the acoustic field which directly impacts the thermoacoustic amplification process. Thus, above the onset and because of nonlinear effects, the temperature distribution (and therefore the acoustic field) deviates unavoidably from the one for which the engine was initially designed. A common solution to counteract these effects is to add passive elements such as membranes [22], jet pumps [1, 22] or tapered tubes [1, 23].

In this paper, our focus is rather oriented to investigate if there is a possibility to control the acoustic field in the thermoacoustic core in order to maximize the process of thermoacoustic amplification. For this purpose, an active control method is used to tune the spatial distribution of the acoustic field by means of an auxiliary acoustic source. This method comes down to drive the self-sustained thermoacoustic oscillation by an external source. Such experimental studies have already been carried out in thermoacoustics. Some studies have focused on the description of the variety of nonlinear dynamics behavior observed in experiments (synchronization [24, 25], route to chaos [26],...). Other studies [27, 28, 29, 30, 31] have focused on the forcing of acoustic oscillations in the context of thermoacoustic engines. In particular, a proof-of-concept study provided by Desjouy et al. [28] in an annular engine has demonstrated that the addition of two auxiliary sources, appropriately tuned, can significantly improve the overall efficiency. More recently, Olivier et al. [31] successfully applied an active control method to the TAEG considered in this paper.

This study carries on with this latter work. The auxiliary source consists of a loudspeaker driven by an electric feedback loop, comprising a phase-shifter and an amplifier, connected to a reference microphone. The novelty lies in the choice of the auxiliary source position, which is located inside the loop-tube just over the main ambient heat exchanger. The aim of this study is to examine the effects of the active control of sound on the TAEG behavior. Experiments show

two main results: the benefit of applying this method in terms of efficiency and temperature gradient at onset, and the existence of a hysteretic behavior leading to a discrepancy between the onset temperature and the offset temperature, caused by the feedback loop itself.

The experimental apparatus is briefly described in section II. The effects of the active control on the system behavior are then analyzed experimentally and compared to the case without active control. Finally, the last section focuses on further discussions about the application of active control feedback loop in thermoacoustic engines and future efforts to improve our understanding of the physical processes responsible for the observed phenomena.

2. Experimental apparatus

The experimental setup is a thermo-acousto-electric generator consisting of a Backhaus-Swift type thermoacoustic engine [1] coupled with an electrodynamic linear alternator, as shown in Fig. 1. It is filled with air at a gauge pressure of 5 bars. **The main geometrical features of the set-up and and the fluid parameters are given in Table 1**. The detailed description of the experimental apparatus can be found in ref. [31] and therefore only a brief description will be provided here.

The torus-shaped section contains a feedback waveguide (42 mm in diameter), a main ambient heat exchanger (AHX_1), a regenerator, a hot heat exchanger (HHX), a thermal buffer tube (TBT) and a secondary ambient heat exchanger (AHX_2). Its unwrapped length is 1.12 m. The regenerator consists of a pile of stainless steel wire-mesh screens. Its porosity is about 69 % and the hydraulic radius of the screen is 20 μm. The ambient heat exchangers are water-cooled to be kept at room temperature $T_c \approx 293$ K, whereas the hot heat exchanger is heated at a hot temperature T_h by a Nichrome resistance ribbon. The inner wall of the part of the torus shaped waveguide (56 mm in diameter) comprised between the two ambient heat exchangers is covered by a ceramic tube in order to reduce the thermal leaks to the outside. The elements of the

Working fluid				
Fluid	Air			
Static pressure	0.5 MPa			
Ambiant temperature	293 K			
Torus Loop				
Component	*Length*	*Diameter*	*Porosity*	*Hydraulic radius*
Feedback waveguide	915 mm	42 mm		
Cone	35 mm			
Compliance	30 mm	56 mm		
AHX_1	15 mm	56 mm	0.60	1 mm (cylindric pore)
Regenerator	23 mm	56 mm	0.85	0.05 mm (mesh grid)
HHX	15 mm	56 mm	0.89	0.30 mm (square pore)
TBT	50 mm	56 mm		
AHX_2	15 mm	56 mm	0.60	1 mm (cylindric pore)
Jonction	22 mm	56 mm		
Coupling waveguide				
Component	*Length*	*Diameter*		
Waveguide	1250 mm	42 mm		
Cone	300 mm			
Alternator back cavity	255 mm	358 mm		

Table 1: Principal fluid and geometrical parameters of the thermoacoustic device.

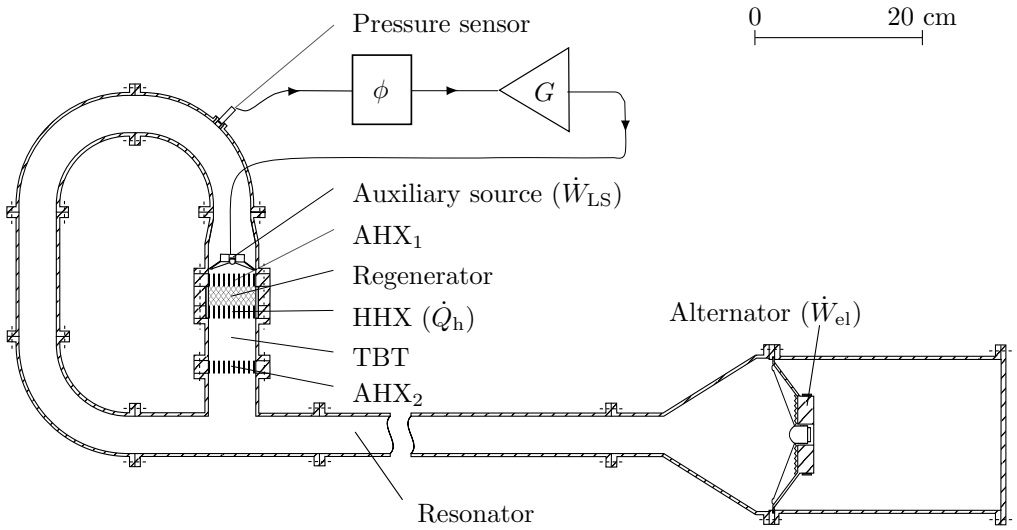

Figure 1: Schematic illustration of the thermo-acousto-electric generator.

torus loop are designed to realize the traveling-wave phasing with high acoustic impedance in the regenerator, as required for a high efficiency thermoacoustic amplification. The torus section is connected via a coupling waveguide (1.55 m in length and 42 mm in diameter) to the alternator and its rear cavity (6.3 l in volume). The alternator is a classical electrodynamic loudspeaker (Monacor SPH-170C). A variable resistor is used to load electrically the alternator in order to extract electrical power $\dot{W}_{\mathrm{el}}$.

The active control system, used to drive the autonomous oscillations, consists of an auxiliary acoustic source, namely an electrodynamic loudspeaker (Aura NSW2-326-8A), powered by the output signal from a pressure sensor μ via the electroacoustic feedback loop which includes a phase-shifter and an audio amplifier. **The phase-shifter consists of three all-pass filter in series.** Thus, the acoustic source input signal is the pressure sensor signal phase-shifted with a phase-shift ϕ and amplified with a voltage gain G. The novelty here compared to the previous study [31] lies in the acoustic source position: it is located inside the loop-tube, whereas it was enclosed in a small cavity and coupled to the loop guide via a capillary tube in the previous study. It is placed just above

the main ambient heat exchanger at a high acoustic impedance position (i.e. large acoustic pressure and low volume velocity), which is suitable for the low displacement of the auxiliary source (its maximal excursion is ±3 mm). Furthermore, the auxiliary source introduces an acoustic load in the engine, whose effect is to increase the heat input which is necessary to trigger the onset of self-sustained oscillations (even when no power is supplied to the auxiliary source), but a model used to describe the onset threshold [11] shows that the heat input rise is the lowest at this position.

All the measurements are done in the steady state regime, which means that between each measurement a time delay is respected until temperature stabilization in the whole device. In order to monitor the temperature, thermocouples are flush-mounted along the device. In particular, two thermocouples measure the temperature difference ΔT between the temperature T_h in the center of the hot heat exchanger and the temperature T_c in the center of the ambient heat exchanger. A piezoelectric pressure sensor, schematically shown in Fig. 1, measures the acoustic pressure above the main ambient heat exchanger. The input heat power $\dot{Q}_\mathrm{h}$ dissipated by Joule effect into the ribbon of the hot heat exchanger is delivered by a DC-power supply (Aim-TTi EX 4210R). The input electric power $\dot{W}_\mathrm{LS}$ supplied to the auxiliary loudspeaker is obtained from the measurement of both the voltage difference and the current (via **an AC current probe**) passing through the moving coil. **Note that the AC current probe was preliminarily calibrated by measuring the current through a 7 Ohm resistor at different frequencies, especially in order to prevent from any source of error related to a phase shift inherent to the probe itself. The maximum input electric power $\dot{W}_\mathrm{LS}$ value is 15 W.** The outgoing electrical power $\dot{W}_\mathrm{el}$ is obtained from the measurement of the voltage difference across the load resistor. The ratio of the outgoing to incoming electrical powers gives the overall efficiency of the engine:

$$\eta = \frac{\dot{W}_\mathrm{el}}{\dot{Q}_\mathrm{h} + \dot{W}_\mathrm{LS}}. \tag{1}$$

In the initial engine without auxiliary source (and so without active control) and for the optimal load resistance ($R_L = 19\ \Omega$) which maximizes the efficiency, the generator starts to oscillate when the heat power $Q_{\mathrm{h,onset}}$ reaches 61 W, which corresponds to a stabilized temperature difference $\Delta T_{\mathrm{onset}}$ across the regenerator of 401.5 K. The onset frequency is about 40 Hz. **In the experiments presented hereafter, the maximum harmonic distortion is less than 3%, meaning that nonlinear effects of propagation due to harmonic cascade of energy are negligible.** For the most efficient case, the maximum thermo-electric efficiency reaches 1 % and the maximum electrical power produced is close to 1 W. Such performance is admittedly limited but can be explained by the fact that the engine is a prototype device working with a moderately pressurized fluid. Nevertheless, the engine has been designed to work in a configuration close to its maximum efficiency point. Moreover, the ultimate goal of this academic work is to demonstrate that an active control method can be advantageously implemented in a thermoacoustic engine, **rather than building a high power/high efficiency engine**.

3. Experimental results

In this section, the objective is to analyze the effects of the active control on the system behavior. Experiments are conducted with active control when we tune the three input parameters of the engine: the heat input Q_{h} and the two parameters controlling the electro-acoustic feedback loop, namely the **imposed** voltage gain G and the **imposed** phase-shift ϕ. Results with active control are compared with those obtained in the initial engine without auxiliary source. The load resistance is fixed at its optimal value which maximizes the efficiency: $R_L = 19\ \Omega$ without active control and $R_L = 23.1\ \Omega$ with active control (the coupling between the auxiliary source and the engine changes the optimal load resistance).

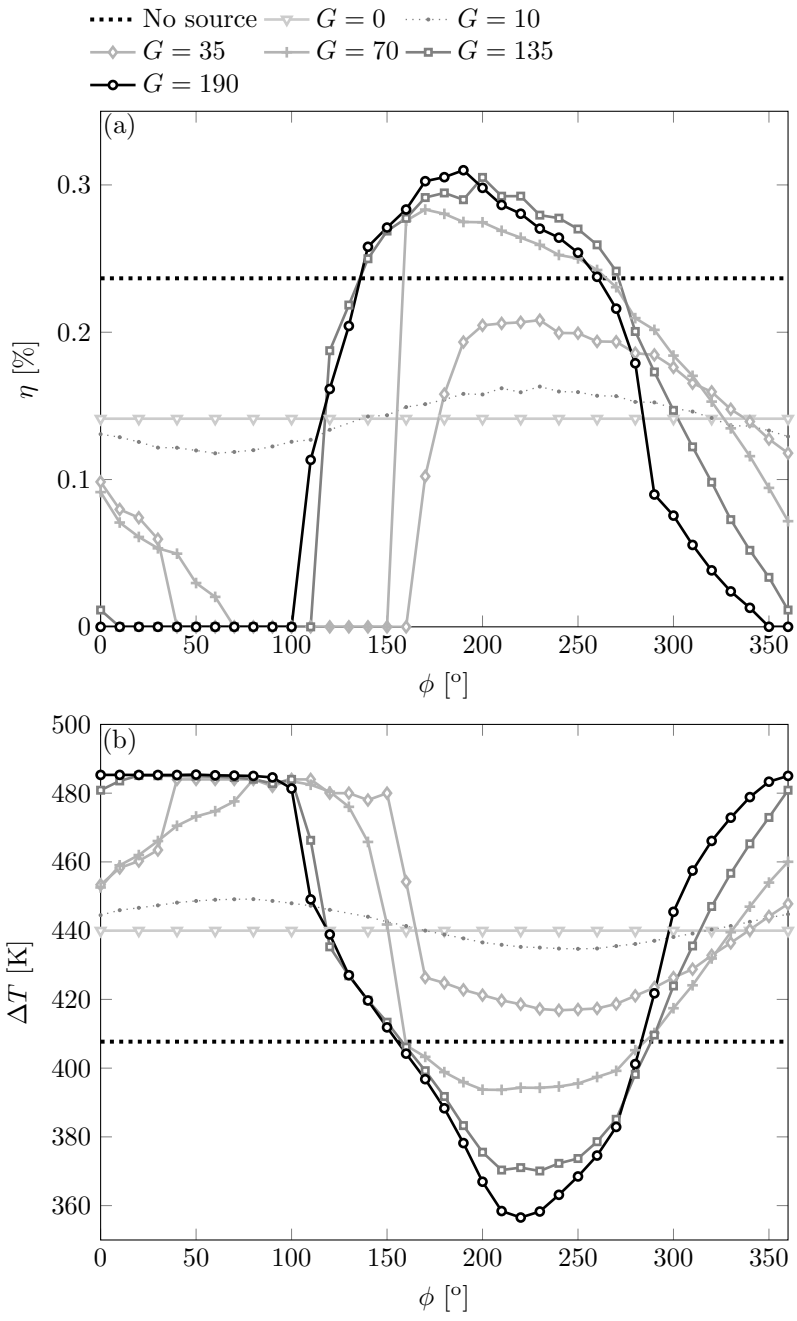

Figure 2: (a) Efficiency η as a function of the **imposed** phase-shift ϕ for different voltage gains G at fixed heat power Q_{h}. (b) Corresponding evolution of the temperature difference ΔT for different voltage gains G. The dotted line corresponds to the initial engine without active control (that is to say, without any source introduced within the closed-loop).

3.1. Effect of phase-shift ϕ for different voltage gains G at fixed heat power Q_{h}

We first look at the influence of the **imposed** phase-shift ϕ on the engine behavior. Measurements are performed for different voltage gains G from 0 to 190, when the heat input Q_{h} is kept constant and fixed at 70 W (above the critical heat input $Q_{\mathrm{h,onset}} = 68$ W for $G = 0$). Figure 2 depicts the efficiency η and the temperature difference ΔT variations as a function of the **imposed** phase-shift ϕ for different voltage gains. The dotted line represents the reference case of the initial engine without active control ($\eta_{\varnothing} = 0.24$ % and $\Delta T_{\varnothing} = 408$ K).

A first observation is that the behavior of the engine is affected by the addition of the auxiliary source. Indeed, when the acoustic source is not powered ($G = 0$), the efficiency drops down whereas the temperature difference increases ($\eta_{G=0} = 0.14$ % and $\Delta T_{\mathrm{G=0}} = 440$ K) compared to the case without active control.

When the acoustic source is powered at a low voltage gain $G = 10$, the efficiency is significantly affected by the tuning of the phase-shift ϕ. The variations of $\eta_{\mathrm{G=10}}$ as a function of ϕ look similar to a sinusoidal amplitude modulation around the constant efficiency $\eta_{\mathrm{G=0}}$.

At higher gains, the efficiency fluctuations versus ϕ deviate from a sinusoidal shape and the phase difference ϕ_{opt} maximizing the efficiency is shifted (e.g. from $\phi_{\mathrm{opt}} = 230$ ° at $G = 10$ to $\phi_{\mathrm{opt}} = 190$ ° at $G = 190$). Moreover, as soon as $G \geq 70$, there exists an optimal phase range $\phi_{\mathrm{opt}} \in [160\ ^{\mathrm{o}} : 260\ ^{\mathrm{o}}]$, for which the resulting thermoelectric efficiency η is higher than the one $\eta_{\varnothing}$ without active control, the maximum efficiency being $\eta = 0.31$ % obtained for $G = 190$ and $\phi = 190$ °, which represents an efficiency improvement of 29 %. The corresponding temperature difference curves illustrate that the efficiency rise occurs with a decrease of the temperature difference, meaning that more acoustic power is generated with a lower temperature gradient, and showing clearly that the thermoacoustic heat pumping by acoustic wave in the regenerator is enhanced. It is important to mention that the temperature difference can decrease below the one without active control. For example, at the maximum efficiency the temperature difference ΔT =356 K is 52 K lower than for the one

corresponding to the initial engine.

It is also worth noting that there exists an "unfavorable" range of value for **the imposed phase-shift** ϕ which even leads to the quenching of self-sustained oscillations (e.g. for $\phi \in [-10\ ^{o} : 100\ ^{o}]$ at $G = 35$ and for $\phi \in [70\ ^{o} : 150\ ^{o}]$ at $G = 190$). In this latter case, the temperature difference ΔT is only controlled by heat diffusion through the thermoacoustic core (no sound, and therefore no heat transport by sound) and it rises to a higher value than in the case when thermoacoustic conversion occurs. Lastly, the phase-shift domain for which the acoustic wave is suppressed extends with the voltage gain.

3.2. Effect of voltage gains G for two heat powers Q_{h} at fixed phase-shift ϕ

To complete these results, experiments are conducted at a constant phase-shift ϕ, when the voltage gain G varies, for two different heat powers: $Q_{\mathrm{h}} = 70$ W and 100 W, respectively just above and away from the onset heat input for $G = 0$ ($Q_{\mathrm{h,onset}} = 68$ W). The phase-shift ϕ is fixed at a value included in the optimal phase range, $\phi = 200\ ^{o}$ and $220\ ^{o}$ respectively for $Q_{\mathrm{h}} = 70$ W and 100 W. Fig. 3 presents the efficiency η and the temperature differences ΔT evolutions with the voltage gain G. As previously observed, for a phase-shift included in the optimal phase range, the gain increase leads to a gradual efficiency increase and a gradual temperature difference decrease. The active control has an interest for both heat powers considered, since the efficiency η increases (by about 30 % for $Q_{\mathrm{h}} = 70$ W and 9 % for 100 W) and the temperature difference ΔT decreases (by about 53 K for $Q_{\mathrm{h}} = 70$ W and 8 K for 100 W) compared to the case without active control (dotted line). However, the impact of the active control is less important for a higher heat input. Moreover, the increase of efficiency saturates when increasing the voltage gain G. In fact, for a high gain or a high input power, the electric power supplied to the auxiliary source becomes significant **(up to 7.6 W at $G = 212$ and $Q_{\mathrm{h}} = 70$ W)** and hence comes to limit the overall efficiency of the engine.

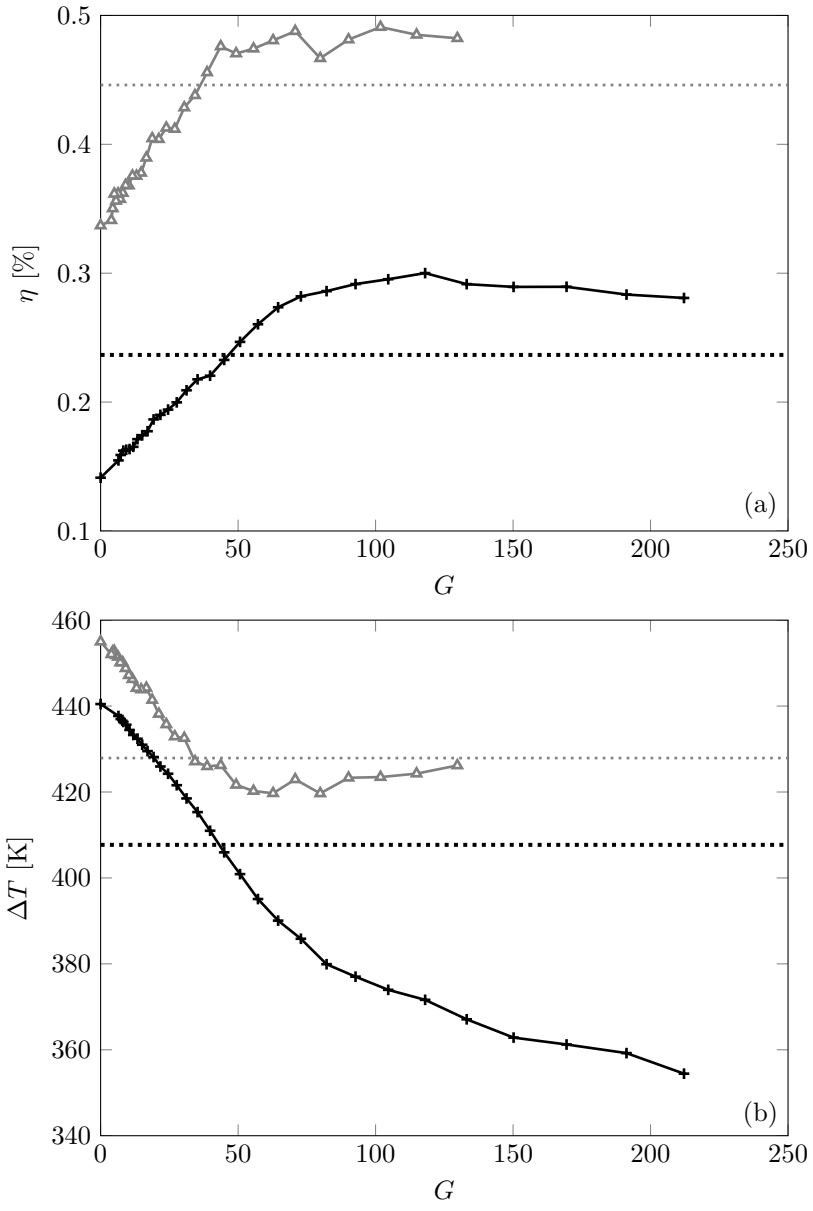

Figure 3: (a) Efficiency η as a function of the voltage gain G for two heat powers Q_{h}= 70 W (+) and 100 W ($\triangle$) at a fixed phase-shift ϕ, respectively 200 $^{\circ}$ and 220 $^{\circ}$. (b) Corresponding evolution of the temperature difference ΔT. The dotted line corresponds to the initial engine without active control (that is to say, without any source introduced within the closed-loop).

3.3. Effect of heat power Q_{h} for different voltage gains G at fixed phase-shift ϕ

The next results concern the observation of the onset and offset of the thermoacoustic instability. Measurements are performed at a fixed phase-shift $\phi = 220\ ^{\mathrm{o}}$ (included in the optimal phase range) and for different gains G with the following protocole: (i) the onset condition ($Q_{\mathrm{h,onset}}$ and $\Delta T_{\mathrm{onset}}$) is determined by increasing the heat input Q_{h} step by step until the acoustic wave generation, (ii) the performance of the engine is characterized for various heat inputs above $Q_{\mathrm{h,onset}}$, (iii) the offset condition ($Q_{\mathrm{h,offset}}$ and $\Delta T_{\mathrm{offset}}$) is determined by decreasing the heat input gradually until the acoustic oscillation death. It is worth pointing out that we took care to wait several minutes between each measurement, in order that the engine has (almost) reached steady-state operation.

The results are presented in Fig. 4. **The onset and offset heat inputs are respectively indicated by triangles and squares and the evolution of the heat input Q_{h} by arrows**. When the source is not powered ($G = 0$), the addition of the auxiliary source leads to the increase of the onset temperature difference and to the decrease of the efficiency compared to the case without active control (dotted line), as previously observed. When the source is powered, i.e. for $G \neq 0$, there exists an hysteresis loop for both the efficiency and the temperature difference behaviors versus the heat input, the offset heat input $Q_{\mathrm{h,offset}}$ becoming lower than the onset heat input $Q_{\mathrm{h,onset}}$ and so leading to a discrepancy between the onset temperature difference and the damping one. The results notably show that once the acoustic wave is initiated, it can be maintained even for $Q_{\mathrm{h}} < Q_{\mathrm{h,onset}}$, meaning that after the engine starts, it can run at a lower temperature difference than its onset one $\Delta T_{\mathrm{onset}}$. It is worth pointing out that this process only occurs if the feedback loop is switched on ($G > 0$). Moreover, the higher the voltage gain G is, the more remarkably the onset heat input and the onset temperature difference are different, respectively from 68 W to 56 W and from 437 K to 343 K, when the gain varies from 0 to 190. At the same time, the offset temperature difference decreases as well from 437 K to 320 K, in such a way that the area of the hysteresis loop increases, meaning

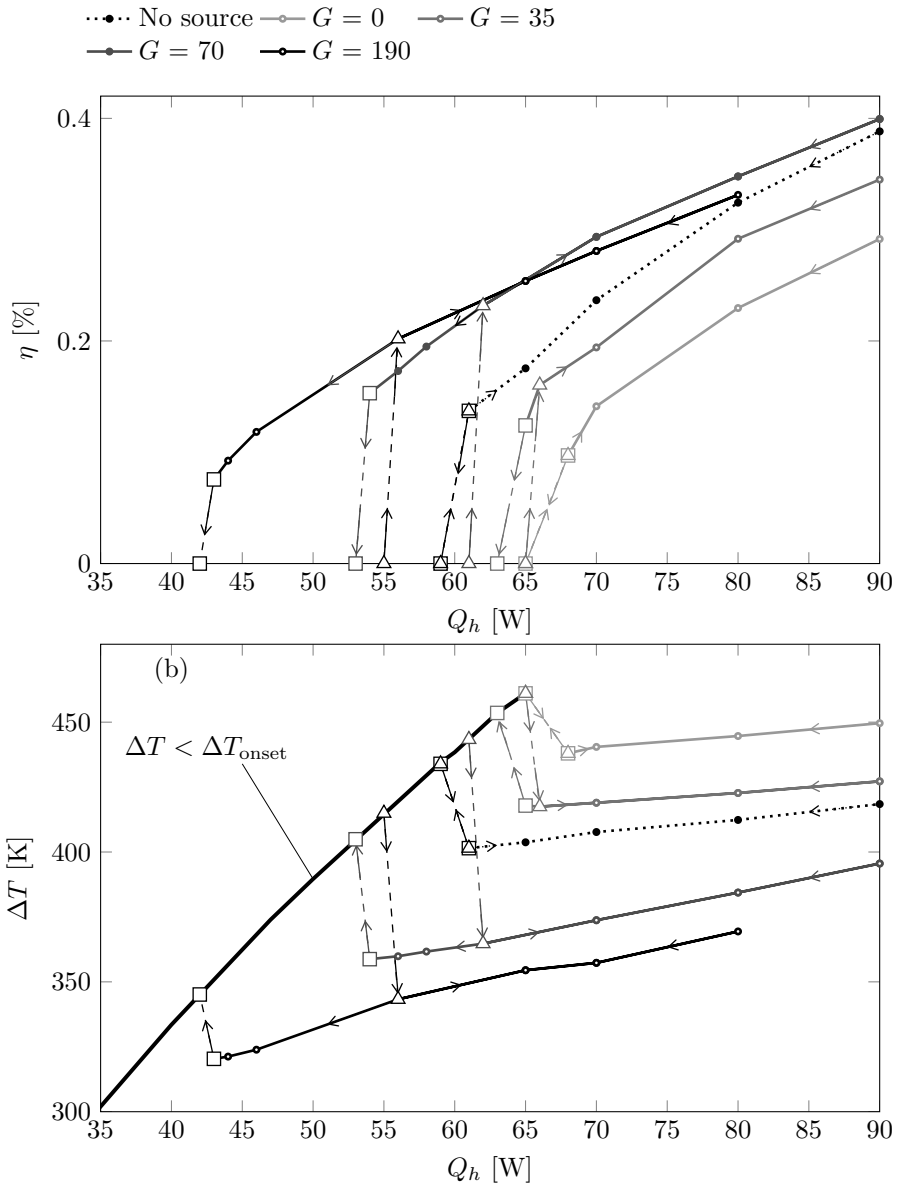

Figure 4: (a) Hysteretic behavior of the efficiency η with the heat input Q_{h}, at a fixed phase-shift $\phi = 220$ ° and for different voltage gains G. (b) Corresponding evolution of the temperature difference ΔT for different voltage gains G. The black line corresponds to the temperature above the onset of thermoacoustic instability. The dotted line corresponds to the initial engine without active control. Arrows indicate the direction of hysteresis. The triangles indicate onset conditions and the squares offset conditions.

that the working temperature range extends toward lower temperatures. This has a major interest since it offers the possibility to upgrade thermal energy at lower temperatures.

4. Discussion

This study was conducted to investigate the effect of an active control method on the behavior of a TAEG. This method consists in forcing the self-sustained thermoacoustic instability with a loudspeaker placed inside the loop-tube in order to control the thermoacoustic amplification. The experimental results highlight that when the auxiliary source is appropriately tuned, some improvements are achieved in terms of efficiency and temperature difference across the regenerator, compared to the case without active control. These observations are consistent with the previous findings [31] observed in a similar setup. However, a major difference comes from the source position, located here inside the loop-tube. At this position, effects of the active control method on the system performance are enhanced in comparison with the previous study, since the efficiency increase reaches at the maximum 30 % with a decrease of the temperature difference of 53 K. Besides, it is also advantageous to place the auxiliary source inside the loop-tube since this suppresses the so-called Gedeon streaming, a second order time-average mass flow running clockwise in the engine (accordingly with Fig.1), which induces an undesired heat flux from the hot heat exchanger to the second ambient heat exchanger (AHX_2). Moreover, a major outcome in comparison with the previous study is the observation of a discrepancy between the onset and the offset temperature which causes a hysteretic behavior of both the temperature difference across the regenerator and the efficiency versus the heat input. As a result, the operating temperature range extends to the lower temperatures. This is an interesting result in the context of waste heat recovery, since this method may offer the possibility to recover heat at a lower temperature and thereby may open up new areas of application.

Although these results seem promising, we have no clear idea at the present time about how the active control affects the engine behavior. One may interpret the results obtained simply by applying the superposition principle, the acoustic power radiated by the auxiliary source being just amplified by the thermoacoustic amplification core. We believe that such an analysis is not sufficient because it could neither explain the presence of quenching nor the hysteretic behavior induced by the electroacoustic feedback loop. Another possibility (hypothesis?) is an indirect modification of the spatial distribution of the temperature field within the thermoacoustic core produced by a change of the acoustic nonlinear effects (for example streaming pattern).

Further studies need to be carried out to get a better understanding of the active control process. The development of a simplified analytic model would provide useful insight to describe the coupling between the thermoacoustic engine and the active control feedback loop and to determine how the active control method operates. This model would also provide a guidance for the selection of an appropriate auxiliary source in the early stage of engine design (in this study, the auxiliary source has been chosen by convenience and a posteriori). Moreover, this study has been performed on a TAEG academic model and the next step will be to experience this active control method in a high power TAEG, which is under construction in our laboratory.

[1] S. Backhaus, G. W. Swift, A thermoacoustic-stirling heat engine: Detailed study, J. Acoust. Soc. Am. 107 (6) (2000) 3148.

[2] M. E. H. Tijani, S. Spoelstra, A high performance thermoacoustic engine, J. Appl. Phys. 110 (9) (2011) 093519–093519–6.

[3] S. Backhaus, E. Tward, M. Petach, Traveling-wave thermoacoustic electric generator, Appl. Phys. Lett. 85 (6) (2004) 1085.

[4] K. De Blok, Novel 4-stage traveling wave thermoacoustic power genera-

tor, in: Proceedings of ASME 2010 3rd joint US-European FEDSM2010-ICNMM2010, American Society of Mechanical Engineers, 2010.

[5] Z. Yu, P. Saechan, A. J. Jaworski, A method of characterising performance of audio loudspeakers for linear alternator applications in low-cost thermoacoustic electricity generators, Appl. Acoust. 72 (5) (2011) 260–267.

[6] D. Zhao, Y. Chew, Energy harvesting from a convection-driven rijke-zhao thermoacoustic engine, J. Appl. Phys. 112 (11) (2012) 114507.

[7] Z. Wu, G. Yu, L. Zhang, W. Dai, E. Luo, Development of a 3 kW double-acting thermoacoustic stirling electric generator, Appl. Energ. 136 (2014) 866–872.

[8] W. C. Ward, G. W. Swift, J. P. Clark, Interactive analysis, design, and teaching for thermoacoustics using DeltaEC, J. Acoust. Soc. Am. 123 (5) (2008) 3546.

[9] A. C. Trapp, F. Zink, O. A. Prokopyev, L. Schaefer, Thermoacoustic heat engine modeling and design optimization, Appl. Therm. Eng. 31 (14-15) (2011) 2518–2528.

[10] N. Rott, Thermally driven acoustic oscillations, part III: Second-order heat flux, Z. Angew. Math. Phys. 26 (1) (1975) 43–49.

[11] M. Guedra, G. Penelet, On the use of a complex frequency for the description of thermoacoustic engines, Acta Acust. United Ac. 98 (2) (2012) 232–241.

[12] H. Yuan, S. Karpov, A. Prosperetti, A simplified model for linear and nonlinear processes in thermoacoustic prime movers. part ii. nonlinear oscillations, J. Acoust. Soc. Am. 102 (6) (1997) 3497–3506.

[13] V. Gusev, H. Bailliet, P. Lotton, M. Bruneau, Asymptotic theory of nonlinear acoustic waves in a thermoacoustic prime-mover, Acta Acust. United Ac. 86 (1) (2000) 25–38.

[14] G. Swift, A. S. of America, Thermoacoustics: A Unifying Perspective for Some Engines and Refrigerators, AIP Conference Proceedings / Atomic, Molecular, Chemical Physics Series, Acoustical Society of America through the American Institute of Physics, 2002.

[15] A. Berson, P. Blanc-Benon, Nonperiodicity of the flow within the gap of a thermoacoustic couple at high amplitudes, J. Acoust. Soc. Am. 122 (4) (2007) EL122–EL127.

[16] J. W. Strutt, On the circulation of air observed in kundt's tubes, and on some allied acoustical problems, Philos. Trans. R. Soc. Lond. 175 (1884) 1–21.

[17] D. Gedeon, Dc gas flows in stirling and pulse tube cryocoolers, in: J. Ross, R.G. (Ed.), Cryocoolers 9, Springer US, 1997, pp. 385–392.

[18] G. P. Smith, R. Raspet, R. Hiller, J. McDaniel, Evanescent modes and anomalous streaming in a thermoacoustic device, Appl. Acoust. 69 (1) (2008) 23–30.

[19] G. Penelet, M. Guedra, V. Gusev, T. Devaux, Simplified account of rayleigh streaming for the description of nonlinear processes leading to steady state sound in thermoacoustic engines, Int. J. Heat Mass Transfer 55 (2122) (2012) 6042 – 6053.

[20] I. Reyt, V. Daru, H. Bailliet, S. Moreau, J.-C. Valire, D. Baltean-Carls, C. Weisman, Fast acoustic streaming in standing waves: Generation of an additional outer streaming cell, J. Acoust. Soc. Am. 134 (3) (2013) 1791–1801.

[21] G. Penelet, S. Job, V. Gusev, P. Lotton, M. Bruneau, Dependence of sound amplification on temperature distribution in annular thermoacoustic engines, Acta Acust. United Ac. 91 (3) (2005) 567–577.

[22] G. W. Swift, D. L. Gardner, S. Backhaus, Acoustic recovery of lost power in pulse tube refrigerators, J. Acoust. Soc. Am. 105 (2) (1999) 711.

[23] J. R. Olson, G. W. Swift, Acoustic streaming in pulse tube refrigerators: tapered pulse tubes, Cryogenics 37 (12) (1997) 769–776.

[24] G. Penelet, T. Biwa, Synchronization of a thermoacoustic oscillator by an external sound source, Am. J. Phys. 81 (4) (2013) 290–297.

[25] T. Yoshida, T. Yazaki, Y. Ueda, T. Biwa, Forced synchronization of periodic oscillations in a gas column: Where is the power source?, J. Phys. Soc. Jpn. 82 (10) (2013) 103001.

[26] T. Yazaki, Experimental observation of thermoacoustic turbulence and universal properties at the quasiperiodic transition to chaos, Phys. Rev. E 48 (1993) 1806–1818.

[27] P. S. Spoor, G. W. Swift, The huygens entrainment phenomenon and thermoacoustic engines, J. Acoust. Soc. Am. 108 (2) (2000) 588–599.

[28] C. Desjouy, G. Penelet, P. Lotton, Active control of thermoacoustic amplification in an annular engine, J. Appl. Phys. 108 (11) (2010) 114904–114904–7.

[29] N. Pan, C. Shen, S. Wang, Experimental study on forced thermoacoustic oscillation driven by loudspeaker, Energ. Convers. and Manage. 65 (0) (2013) 84–91.

[30] S. Li, D. Zhao, Heat flux and acoustic power in a convection-driven t-shaped thermoacoustic system, Energ. Convers. and Manage. 75 (2013) 336–347.

[31] C. Olivier, G. Penelet, G. Poignand, P. Lotton, Active control of thermoacoustic amplification in a thermo-acousto-electric engine, J. Appl. Phys. 115 (17) (2014) 174905.